Title: Effects of urbanization on cloud-to-ground lightning strike frequency: a global perspective

J. Pablo Narvaez[1,2*], Stephen P. Yanoviak[1,3], Phillip M. Bitzer[4], Jeffrey C. Burchfield[5], Evan M. Gora[1,6]

[1] Smithsonian Tropical Research Institute, Apartado 0843-03092, Balboa, Panama
[2] Department of Biological Sciences, Marquette University, Milwaukee, WI, 53201, USA
[3] Department of Biology, University of Louisville, 139 Life Sciences Building, Louisville, KY, 40292, USA
[4] Department of Atmospheric and Earth Science, The University of Alabama in Huntsville, Huntsville, AL, 35899, USA
[5] Earth System Science Center, The University of Alabama in Huntsville, Huntsville, AL, 35899, USA
[6] Cary Institute of Ecosystem Studies, Millbrook, New York, NY, 12545, USA

*Corresponding author, email: pablo.narvaez@marquette.edu

Key Points

- Urban lightning enhancement is common and often very strong, but not all cities exhibit enhancement.
- Lightning enhancement is influenced by urban heat island effects, enhanced local precipitation, and regional lightning frequency.
- Likelihood and strength of enhancement were marginally increased in larger cities at lower latitudes, elevations, and distances to water.

Abstract

Urbanization tends to increase local lightning frequency (i.e., the "lightning enhancement" effect). Despite many urban areas showing lightning enhancement, the prevalence of these effects is unknown, and the drivers underlying these patterns are poorly quantified. We conducted a global assessment of cloud-to-ground lightning flashes (lightning strikes) across 349 cities to evaluate how the likelihood and magnitude of lightning enhancement vary with geography, climate, air pollution, topography, and urban development. The likelihood of exhibiting lightning enhancement increased with higher temperature and precipitation in urban areas relative to their natural surroundings (i.e., urban heat islands and elevated urban precipitation), higher regional lightning strike frequency, greater distance to water bodies, and lower elevations. Lightning enhancement was stronger in cities with conspicuous heat island and elevated urban precipitation effects, higher lightning strike frequency, larger urban areas, and lower latitudes. The particularly strong effects of elevated urban temperature and precipitation indicate that these are dominant mechanisms by which cities cause local lightning enhancement.

Keywords: lightning enhancement, urban systems, remote sensing, urban heat island, model averaging

1. Introduction

Lightning, particularly discharges that strike the ground (i.e., cloud-to-ground lightning), is an agent of death and destruction in natural and anthropogenic systems. Local lightning frequency increases with higher temperatures, greater fine aerosol concentrations, proximity to water bodies, and the presence of tall, isolated objects (Westcott, 1995; Steiger *et al.,* 2002; Naccarato *et al.,* 2003; Table 1). Many cities provide this exact combination of ingredients, and local lightning frequency tends to be higher in urban areas – a phenomenon referred to as the lightning enhancement effect (Orville et al., 2001; Naccarato *et al.,* 2003; Table 1). However, evidence for lightning enhancement is limited to a relatively small number of cities, and the mechanisms are either unclear or unknown in most cases. Fundamentally, because these studies compare one or a few cities to nearby landscapes that differ in a multitude of ways, the resulting patterns are confounded by multiple variables, including both measured and unmeasured factors. Thus, this study aimed to overcome these limitations by exploring global variation in lightning enhancement to determine (1) how widespread is the positive effect of urbanization on regional lightning strike frequency, and (2) what characteristics of cities are most strongly associated with variation in the lightning enhancement effect.

Lightning enhancement is linked to air pollution and elevated temperatures associated with urban areas (Table 1). Anthropogenic and naturally derived aerosols (e.g., sulfate and nitrate aerosol products from the combustion of fossil fuels, and sea spray aerosols or volcanic ash, respectively) can alter within-cloud processes to increase lightning frequency (Twomey *et al*., 1984; Yau & Rogers, 1996; Stolz, 2016; Thornton *et al.,* 2017). Similarly, the urban heat island effect (i.e., the tendency for cities to be hotter than nearby natural environments; Oke, 1982) can increase convection, thereby increasing lightning activity (Bornstein & Lin, 2000). Although lightning enhancement is often statistically linked to aerosol concentrations or urban heat islands (9 of 12 studies for aerosols and 3 of 4 studies for urban heat islands; Table 1; Soriano & de Pablo, 2002; Kar *et al*., 2007, 2009), these factors are inherently confounded with other aspects of urbanization. Associations with these factors are unknown for most cities lacking lightning enhancement, perhaps due to the limited number of cities studied and potential biases in city selection (e.g., 100% of single city studies reported enhancement, whereas 76.7% of cities exhibited enhancement in multi-city studies; Table 1). This study addresses this problem by examining a large number of cities spanning wide variation in pollution, heat island effects, and lightning enhancement.

Lightning enhancement also is influenced by geography, topography, and associated climatic patterns. On a global scale, lightning frequency is highest near the equator, where temperatures and rainfall rates also tend to be high (Christian *et al*., 2003). At more local geographic scales, lightning frequency tends to be high near water bodies (Song *et al.,* 2004; Freitas *et al.,* 2007; Holle & Murphy, 2017), presumably due to abundant moisture and higher concentrations of fine particulate aerosols. Similarly, lightning frequency is particularly high in the foothills of some montane regions (Mushtaq *et al*., 2018), indicating that topography influences lightning activity. These factors potentially interact with temperature and air pollution near urban centers to modulate the likelihood and magnitude of the lightning enhancement effect.

However, the contribution of some of these factors (e.g., urban topography, population) is typically overlooked in urban lightning research (Burke & Shepherd, 2023).

Apart from these mechanistic drivers, the best predictors of urban lightning enhancement effects may be metrics of urbanization. Ultimately, the lightning enhancement effect is linked to urban development and its impact on the local climate. Thus, critical metrics of urban development, such as urban area, population size, or the density of urbanization (i.e., the extent of natural cover within the urban areas), likely predict variation in the lightning enhancement effect (e.g*.,* Kar & Liou 2019; Soriano & Pablo, 2002). However, these relationships are untested.

Here, we quantify the distribution of urban lightning enhancement among 349 cities worldwide and explore the factors influencing the magnitude of enhancement. Specifically, we evaluate how urbanization influences lightning frequency within the boundaries of each city. Based on existing data and hypotheses described above, we predicted that urban lightning enhancement is more common and stronger where (1) urban heat islands are hotter, (2) air has higher aerosols and particulate concentrations associated with pollution, (3) urban areas are closer to water bodies, and (4) cities cover more area or have greater populations. This study is unique in scope and scale because it captures global variation in urbanization and its effects on lightning enhancement. This approach does not measure physical processes within individual cities. However, it is unprecedented in its scale and, thus, its statistical power to separate the contributions of potentially confounding effects on lightning enhancement.

2. Methods

2.1.Lightning strike data

We quantified the urban lightning enhancement effect using Earth Networks Total Lightning Network (ENTLN) data. ENTLN continuously detects and locates lightning using each discharge's time and signal amplitude (Liu & Heckman, 2012); here, we focus on the ENTLN-classified cloud-to-ground flashes (or a group of strokes), which we call lightning strikes. We omitted lightning strikes <10 kA in magnitude to avoid misclassification with in-cloud lightning (Cummins *et al.,* 1998). We calculated monthly mean lightning strike frequency (lightning strikes km^{-2} yr^{-1}) on a 0.05×0.05-degree grid (ca. 5×5 km) extending from 60°N to 60°S latitude for 2013-2020.

2.2.Urban and natural areas

We used the 2018 Moderate Resolution Imaging Spectroradiometer (MODIS) land cover data (MCD12C1 Version 6; Friedl & Sulla-Menashe, 2019) on a 0.05-degree grid to identify urbanized land and its surrounding natural areas. The operational definition of a city used in this study was >300,000 inhabitants, based on the definition of a city in the UN World Urbanization Prospects (UN, 2018). We did not differentiate among various definitions of urban areas (e.g., city proper, urban agglomeration, metropolitan area), which likely introduces additional variation. Regardless, these were the best data available and suitable for capturing broad trends in population size. We omitted only five cities by limiting the data to within 60°N and 60°S latitude. Additionally, we did not evaluate the increase or decrease in the urban area during the

2013-2020 period. We assumed that the changes in area in most cities in the last decade are not significant enough to influence the lightning enhancement effect. Spatially, we defined cities as clusters of 0.05 x 0.05-degree cells with more than 50% urbanization overlapping the city center, defined by the United Nations World's Cities in 2018–Data Booklet (UN, 2018), or contiguous with other urban cells. Because the urbanization footprint of a city is often a mosaic of developed and undeveloped space (e.g., water bodies), we also included any cell with >50% urban area that was within two cells of the city center or contiguous city area (no cells of <50% urban area were included in a city). These adjacent and nearby urban cells collectively represented the urban area for each city (Fig. S1a-c). This process collapsed 22 pairs of cities into a single urban center (e.g., Dallas/Ft. Worth, Philadelphia/Trenton). We identified 884 cities with >300,000 inhabitants and at least one cell comprising >50% urban area.

We used MODIS to identify *natural areas* surrounding each city. Specifically, we defined natural areas as any combination of non-modified MODIS terrestrial layers: mixed forest, evergreen needleleaf forest, evergreen broadleaf forest, deciduous needleleaf forest, deciduous broadleaf forest, woody savannas, savannas, grasslands, closed shrublands, open shrublands, permanent wetlands, permanent snow, and barren land (excluding water bodies, urban area, and croplands) within 150 km of the boundaries of a city. We chose a 150 km radius because it is ca. 1/10 of the detection distance of this sensor system and therefore should experience limited bias in detection efficiency across its area. Additionally, a buffer of 150 km captures sufficient area to estimate non-urban lightning frequency, and this radius was previously used to assess climatic differences between urban and non-urban pairs (e.g., urban island effect and pollution; He et al., 2007; Mendez-Espinosa et al., 2019). When a cell was within 150 km of multiple cities, we associated that natural area cell with the closest city. To limit edge effects, we removed all natural areas within two cells (ca. 10 km) of any cell with >50% urban area (Fig. S1d). We only retained cities in our dataset if they had at least 100 km^2 of associated natural area (691 cities qualified; Fig. S2c). The natural areas capture typical lightning frequency of each region with limited direct influence of urbanization, functioning as a reference point for evaluating the effect of each urban area.

2.3.Calculating lightning frequency

We calculated each pixel's average (i.e., the mean) annual lightning frequency using only months with meaningful lightning activity. We removed all cities with < 1 lightning strike km^{-2} yr^{-1} in their associated natural areas. We also removed months from individual cities if their natural areas exhibited < 1 lightning strike km^{-2} yr^{-1} in those months (328 cities removed). This approach was necessary for two reasons. First, we lacked the statistical power to test for urban enhancement when lightning frequency is low because lightning frequency is strongly overdispersed and within-city sample sizes were small. Second, removing low-frequency months avoided spurious effects resulting from uneven seasonality patterns (e.g., including all months would produce a latitudinal effect relating to season rather than the strength of urban enhancement). Additionally, we removed months and cities (8 cities in total) lacking data for their covariates (e.g., precipitation data was not available for 2019 and 2020, and the aerosol

optical depth sensor could not make its measurement in certain areas during the study). Following these criteria, we ultimately included 349 cities in the analyses.

We used Glass's delta effect size and a simulation approach to evaluate whether each city exhibited unambiguous lightning enhancement. Glass's delta effect size is a statistical method for quantifying the magnitude of the difference between a treatment group (here, an urban area) and a control (nearby natural areas). To calculate Glass's delta, we divided the mean difference in lightning strike frequency (lightning strikes km^{-2} yr^{-1}) between urban and natural areas by the standard deviation of lightning strike frequency of the associated natural area. Glass's delta was preferable to other effect size metrics because the much larger sample size of the natural areas, relative to the cities, results in a more precise estimate of standard deviation (Fig. S2a-c). Effect sizes ≥0.5 were considered significant (Cohen, 1992). We confirmed that 218 of the 228 cities with effect sizes >0.5 were also identified as significant using a simulation test based on random pulls from the natural area associated with each city. Specifically, we calculated the mean lightning strike frequency for random pulls of natural area cells (10,000 repetitions with the number of resampled natural cells equal to the number of urban cells). We confirmed that <5% of repetitions had an average lightning frequency equal to or greater than the observed lightning frequency in the urban area. We considered the 218 cities identified with both approaches as those exhibiting unambiguous lightning enhancement. This conservative approach likely eliminated false positives while potentially producing some false negatives.

The detection efficiency of ENTLN likely exhibits unquantifiable spatial biases. However, the spatial grain of these biases is much larger than that of our city and natural area measurements (150 km radius) because individual ENTLN sensors detect lightning over distances >1000 km. Moreover, changes in network sensitivity over time will be experienced similarly by all city-specific pixels because of their proximity. We measured the strength of urban enhancement by dividing a city's average lightning strike frequency by the average lightning strike frequency in its associated natural area (hereafter, *urban-natural strike ratio*). Accordingly, this approach is insensitive to possible differences in detection efficiency among cities or over time.

2.4.Climatological, topographical, and geographic covariates

We used spatially explicit, gridded data products to aggregate climatological, topographical, and geographic covariates for each 0.05 x 0.05-degree cell (Table 2). We assigned each 0.05 x 0.05 cell the proportional average of overlapping sulfur dioxide (SO_2) values because of the mismatch in resolution. All other data were downscaled or upscaled to the same spatial grain as the lightning data (Table 2). Climate and pollution data were aggregated monthly. The temperature metrics captured monthly averages of daily trends and were advantageous because of their broad spatial coverage and fine resolution, but they did not capture detailed within-day variation, which could influence both rainfall and lightning activity (Sheperd et al., 2015). All other variables had a single value because they did not change during the study period (e.g., topography) or data were limited (e.g., population).

We used these spatially explicit datasets to calculate potential predictors of variation in the lightning enhancement effect. For each variable described in Table 2, we extracted its average value for each urban area during the months retained in the dataset (i.e., months with > 1 lightning strike km^{-2} yr^{-1}). We calculated annual and cumulative averages of those values from 2013-2020. The only exception was regional lightning frequency, which equaled the mean lightning strike frequency across all natural and urban cells (i.e., the region). To assess the density of urbanization within each city, we calculated the percentage of land covered by natural areas within the urban cells of each city (hereafter, *greenspace*). We also calculated the local effect of urbanization on temperature, precipitation, and all aerosol variables. Specifically, we divided the average values of these predictors in the urban areas by their average across all cells in the associated natural areas, and we referred to these variables as the "variable" ratio (e.g., temperature ratio or precipitation ratio). This allowed us to determine if lightning enhancement was directly associated with the effect of urbanization on local climate and pollution, such as the urban heat island effect (i.e., urban temperature divided by natural area temperature). We log-transformed overdispersed variables before analysis (12 of the 17 fixed-effect predictors were transformed; average temperature, local precipitation, total elevation, absolute latitude, and greenspace were not transformed). Because the annual data for aerosol depth and urban-natural strike ratio included 3 and 4 zero values, respectively, we added half the smallest positive value (0.0020 for aerosol optical depth and 0.0446 for urban-natural strike ratio) to each variable before transformation.

2.5.Model averaging

We used Akaike Information Criterion (AIC) model averaging to explore spatiotemporal variation in the likelihood and magnitude of the lightning enhancement effect. This statistical method fits all possible models from the set of predictors and then blends predictions from the best-performing candidate models based on their goodness-of-fit (i.e., AIC scores), ultimately identifying fixed effects that consistently explain variation in the response variable. To evaluate the probability of enhancement, we constructed a generalized linear model with a binary response variable indicating whether there was lightning enhancement (determined by a threshold of Glass' delta ≥ 0.5). This model included a single value for each city with 17 predictors averaged across all years (349 observations; Table 2). To explore spatiotemporal variation in enhancement strength, we assessed how the urban-natural strike ratio varied among cities with unambiguous enhancement using annual data from 2013-2018 (218 cities with 1,217 city-year observations). Specifically, we constructed a mixed-effect linear model (fitted with the lmer function of the lme4 package; Bates et al., 2015) with an urban-natural strike ratio as the response variable, a random effect for the city (accounting for the annual lightning variation of each city), and the same collection of 17 fixed-effect predictors (Table 2; representing the linear relationships between these predictors and the response variable). We used unique annual values for all variables with yearly data (i.e., all lightning, climate, and pollution variables). We note that some variables were omitted from this final set of predictors (i.e., mean maximum temperature, mean minimum temperature, the ratios between urban and natural areas for these two variables, and the total concentration of NO_2) because of collinearity, as determined by Pearson correlations ($R > 0.7$) and variance inflation factors ($VIF > 5$).

We fitted models for every possible combination of these terms (function *dredge*). Then, we averaged all models with AICc values within 4 of the lowest AICc values (function *model.avg* in package MuMIn; Barton, 2010). We scaled all variables (Z-transformation) to allow direct comparison of coefficients, and we identified significant predictors as model-averaged coefficients with 95% confidence intervals that did not overlap with zero. Additionally, we performed forward model selection and assessed whether including pairwise interaction terms between the significant predictors decreased model AIC. We verified the appropriate model fit and the need for all transformations by evaluating model residuals (e.g., Q-Q plots). All analyses were conducted in the R statistical environment (R Core Team, 2013).

3. Results

Among the 349 cities with ≥ 1 lightning strike km^{-2} yr^{-1}, 218 exhibited unambiguous lightning enhancement based on the criteria used in this study (Fig. 1a-b). The likelihood of exhibiting unambiguous lightning enhancement increased with increasing regional lightning strike frequency, stronger urban heat island effects, higher precipitation ratios (i.e., local precipitation divided by natural area precipitation), larger distance to water bodies, and lower elevation (Fig. 2, Fig. 3a-e, Table S1, Table S3). However, the likelihood of enhancement was not associated with average temperature, local precipitation, pollution, other topographic and geographic variables, or any metrics of urbanization. There were no interactions among the significant predictors identified with model averaging.

The effects of lightning enhancement were particularly strong in some cities. Urban lightning strike frequency was more than double nearby natural areas in 46.8% of cities with enhancement (102 of 218), with a maximum of 10 times more lightning strikes in the urban area of Baoding, China, compared to its natural surroundings in 2020 (16.2 vs. 1.6 lightning strikes km^{-2} yr^{-1} in its urban and natural area, respectively; Fig. 2f). Among cities with significant lightning enhancement, the urban-natural strike ratio (i.e., the magnitude of enhancement) increased with higher regional lightning strike frequency, strong urban heat island effects, higher precipitation ratios, larger urban areas, and at lower latitudes. However, the strength of urban lightning enhancement did not change with pollution, other climate and topographic variables, or other urban characteristics (Fig. 2; Fig. S3a-d, Table S1, Table S3).

The effects of higher precipitation ratios (i.e., urban precipitation relative to their natural areas) and urban area were modified by interactions with other variables (Fig. S4a-c, Table S1, Table S3). The impact of increased precipitation ratios on the strength of lightning enhancement was greater in regions with higher overall lightning strike frequency and among cities located in higher latitudes. By contrast, the effect of urban area on the strength of lightning enhancement was lessened in regions with high lightning strike frequency. There were no significant interactions among other predictors.

4. Discussion

Here, we provide the first global assessment of urban lightning enhancement and its drivers. Increased local lightning strike frequency occurred in at least 218 major cities worldwide, with extremely strong effects in a subset of those cities. However, we also show that

not all urban areas had detectable lightning enhancement effects. The results indicate that urban heat island effects disproportionately influence lightning enhancement, potentially by altering storm activity. These patterns improve our understanding of how cities change local climate and highlight potential avenues for mitigation.

The results of this study support the prediction that urban heat island effects influence lightning enhancement; however, we found no evidence that pollution increases lightning strike frequency in urban areas. Our approach could underestimate the cumulative effects of pollution by ignoring lightning enhancement in nearby natural areas. Nonetheless, when considering lightning enhancement over cities themselves, our global analysis effectively separates the contributions of many varied factors, revealing that urban heat island effects are stronger and more consistent than the effects of pollution. Urban heat island effects can disrupt atmospheric stability, leading to thunderstorms due to the increased convection of air masses (Naccarato et al., 2003). Because urban heat island effects are dependent on urban design, efforts to reduce urban heat islands via shifts in urban planning (e.g., green roofs, building orientation, or construction materials; Shahmohamadi et al., 2010; Changnon, 1992; Shepherd et al., 2015) may also reduce lightning enhancement. Unraveling the mechanisms underlying urban heat island effects on lightning enhancement requires a detailed exploration of the physical processes of lightning initiation.

Both regional lightning strike frequency and the differences in precipitation between urban and surrounding natural areas shape lightning enhancement patterns. The effect of regional lightning strike frequency on lightning enhancement suggests that urbanization primarily amplifies lightning frequency where it already occurs rather than creating lightning where it is uncommon. Additionally, the higher rates of lightning enhancement among cities that also exhibited higher precipitation ratios (presumably caused by anthropogenic factors such as urban aerosols; Shepherd et al., 2015), indicate that urbanization could increase lightning strike frequency, in part, by producing more or stronger storms (Bornstein & Lin, 2000; Baik *et al.,* 2001; Rozoff *et al.,* 2003; Wang, 2005; Van den Heever *et al.,* 2006; Martins, 2009; Thielen *et al.,* 2000). Our metric of increased precipitation ratios does not directly measure convection, but it likely captures differences in convective rainfall and overall storm activity. We need further investigation into urbanization, lightning, and storm formation to understand the processes underlying these relationships.

Aspects of geography, topography, and urbanization also influenced lightning enhancement. These effects suggest that large, lowland cities in tropical regions are the most susceptible to strong lightning enhancement effects. Predictions of future urbanization suggest an increased number of large cities in tropical areas (Gupta, 2002), many of which will be at low elevations. Thus, these cities will be particularly likely to produce strong lightning enhancement effects. Cities at low elevations typically have higher temperatures than high-elevation cities, which may exacerbate urban heat island effects on lightning enhancement. Counter to our expectations, coastal cities exhibit less lightning enhancement than inland cities. One possible explanation is that coastal cities exhibit less temperature variation than inland cities due to the thermal buffering of the ocean (Pamarthi, 2019), and fast temperature changes (which were not

captured in this study) could produce both more thunderstorms and stronger urban heat island effects (Lal & Pawar, 2011). However, this effect was particularly weak and was not apparent in the bivariate analyses or the enhancement strength. Urban planning to reduce urban heat island effects, which has many other benefits, could also reduce the likelihood of lightning enhancement among these growing cities.

The results of this study suggest at least three avenues for further research that would improve our understanding of anthropogenic effects on lightning frequency and distribution. First, large-scale studies of local-scale atmospheric phenomena across more cities could validate the global-scale trends of lightning enhancement in our study (Table 1). Second, the effects of urbanization on lightning characteristics (e.g., the fraction of flashes that are ground strikes and the intensity of individual discharges) remain unknown. Finally, examining lightning enhancement among smaller-scale geographic features (e.g., the relevance of urban greenspace) and beyond the boundaries of urban limits (e.g., downwind effects of urbanization) could inform urban planning decisions. Ultimately, continued monitoring will be crucial to understanding how humans shape regional atmospheric phenomena and how those effects will respond to global change.

Acknowledgments

The Smithsonian Tropical Research Institute (STRI) provided logistical support. This work was partially funded by an STRI Earl S. Tupper Fellowship and by grants from the National Science Foundation (DEB-2213246 to S.P.Y.; DEB-2213247 to P.B.; and DEB-2213245 to E.M.G.). The authors declare no conflicts of interest relevant to this study.

Author's Contributions

P.N. and E.M.G designed the study. P.N. assembled the datasets, and P.N. and E.M.G. analyzed the data. P.N. led the writing of the manuscript. P.B. and J.B. processed the global lightning data. All authors contributed to the conceptual development and writing of the manuscript.

Data Availability Statement

Data and code will be made publicly available via the Cary Institute Figshare. [Dataset] Earth networks provide lightning data, which are not publicly available. [Dataset] CHELSA V2 climatic monthly time series were used to assess the temperature and precipitation data (Karger *et al*., 2017), available at https://envicloud.wsl.ch/#/?prefix=chelsa%2Fchelsa_V2%2FGLOBAL%2F. [Dataset] Terra/MODIS Aerosol Optical Depth monthly time series (Kaufman *et al*., 2002) were downloaded from https://neo.gsfc.nasa.gov/view.php?datasetId=MODAL2_M_AER_OD. [Dataset] Aura Nitrogen Dioxide monthly time series (Krotkov *et al.,* 2016) are available at https://neo.gsfc.nasa.gov/view.php?datasetId=AURA_NO2_M. [Dataset] Modern-Era Retrospective analysis for Research and Applications version 2 (MERRA-2) Sulfate Dioxide monthly time series (Gelaro *et al.,* 2017) can be found at https://disc.gsfc.nasa.gov/datasets/M2TMNXAER_5.12.4/summary. [Dataset] Global Solar Atlas terrain elevation data (Solargis, 2019) can be downloaded

from https://solargis.com/es/maps-and-gis-data/download/world. [Dataset] Global Oceans and Seas shapefile to measure the distance to water bodies (Flanders Marine Institute, 2021) was downloaded from https://www.marineregions.org/downloads.php#seavox. [Dataset] The urban area and greenspace were obtained from the Moderate Resolution Imaging Spectroradiometer (MODIS) Land Cover Climate Modeling Grid (CMG) (MCD12C1) Version 6.1 (Friedl & Sulla-Menashe, 2019) in https://lpdaac.usgs.gov/products/mcd12c1v061/. [Dataset] The Annual Population of Urban Agglomerations with 300,000 Inhabitants or More in 2018 by country, 1950-2035, was downloaded from the World Urbanization Prospects 2018 (UN, 2018) and found at https://population.un.org/wup/Download/.

5. REFERENCES:

Ackerman, A. S., Toon, O. B., Stevens, D. E., Heymsfield, A. J., Ramanathan, V., & Welton, E. J. (2000). Reduction of tropical cloudiness by soot. *Science*, *288*(5468), 1042–1047. https://doi.org/10.1126/science.288.5468.1042

Baik, J.-J., Kim, Y.-H., & Chun, H.-Y. (2001). Dry and moist convection forced by an urban heat island. *Journal of Applied Meteorology*, *40*(8), 1462–1475.

Barton, K. (2010). MuMIn: multi-model inference. R package version 0.13. 17. *Http://CRAN. R-Project. Org/Package= MuMIn*.

Bates, D., Maechler, M., Bolker, B., Walker, S., Christensen, R. H. B., Singmann, H., ... & Bolker, M. B. (2015). Package 'lme4'. *convergence*, 12(1), 2.

Bornstein, R., & Lin, Q. (2000). Urban heat islands and summertime convective thunderstorms in Atlanta: Three case studies. *Atmospheric Environment*, *34*(3), 507–516.

Burke, J. D., & Shepherd, M. (2023). The urban lightning effect revealed with geostationary lightning mapper observations. *Geophysical Research Letters*, 50(6), e2022GL102272.

Changnon, S. A. (1992). Modification in Urban Areas : Lessons for Global Climate Change. *Bulletin of the American Meteorological Society*, *73*(5), 619–627.

Christian, H. J., Blakeslee, R. J., Boccippio, D. J., Boeck, W. L., Buechler, D. E., Driscoll, K. T., Goodman, S. J., Hall, J. M., Koshak, W. J., Mach, D. M., & others. (2003). Global frequency and distribution of lightning as observed from space by the Optical Transient Detector. *Journal of Geophysical Research: Atmospheres*, *108*(D1), ACL--4.

Cohen, J. (1992). Quantitative methods in psychology: A power primer. *Psychological Bulletin*.

Cummins, K. L., Murphy, M. J., Bardo, E. A., Hiscox, W. L., Pyle, R. B., & Pifer, A. E. (1998). A combined TOA/MDF technology upgrade of the US National Lightning Detection Network. *Journal of Geophysical Research: Atmospheres*, *103*(D8), pp. 9035–9044.

den Heever, S. C., Carrió, G. G., Cotton, W. R., DeMott, P. J., & Prenni, A. J. (2006). Impacts of nucleating aerosol on Florida storms. Part I: Mesoscale simulations. *Journal of the Atmospheric Sciences*, *63*(7), 1752–1775.

Flanders Marine Institute. (2021). *Maritime boundaries geodatabase: maritime boundaries and exclusive economic zones (200NM), version 11* [Dataset]. https://www.marineregions.org

Freitas, E. D., Rozoff, C. M., Cotton, W. R., & Silva Dias, P. L. (2007). Interactions of an urban heat island and sea-breeze circulations during winter over the metropolitan area of São Paulo, Brazil. *Boundary-Layer Meteorology*, *122*(1), 43–65. https://doi.org/10.1007/s10546-006-9091-3

Friedl, M., & Sulla-Menashe, D. (2019). MCD12Q1 MODIS/Terra+ aqua land cover type yearly L3 global 500m SIN grid V006 [Dataset]. *NASA EOSDIS Land Processes DAAC*, pp. *10*, 200. https://lpdaac.usgs.gov/products/mcd12q1v006/

Gelaro, R., McCarty, W., Suárez, M. J., Todling, R., Molod, A., Takacs, L., Randles, C. A., Darmenov, A., Bosilovich, M. G., Reichle, R., Wargan, K., Coy, L., Cullather, R., Draper, C., Akella, S., Buchard, V., Conaty, A., da Silva, A. M., Gu, W., … Zhao, B. (2017). The modern-era retrospective analysis for research and applications, version 2 (MERRA-2) [Dataset]. *Journal of Climate*, *30*(14), 5419–5454. https://doi.org/10.1175/JCLI-D-16-0758.1

Gupta, A. (2002). Geoindicators for tropical urbanization. *Environmental Geology*, *42*(7), 736–742.

He, J. F., Liu, J. Y., Zhuang, D. F., Zhang, W., & Liu, M. L. (2007). Assessing the effect of land use/land cover change on the change of urban heat island intensity. *Theoretical and applied climatology*, 90, 217-226.

Holle, R. L., & Murphy, M. J. (2017). Lightning over three large tropical lakes and the strait of Malacca: Exploratory analyses. *Monthly Weather Review*, *145*(11), 4559–4573. https://doi.org/10.1175/MWR-D-17-0010.1

Kar, S. K., Liou, Y.-A., & Ha, K.-J. (2007). Characteristics of cloud-to-ground lightning activity over Seoul, South Korea in relation to an urban effect. *Annales Geophysicae*, *25*(10), 2113–2118.

Kar, S. K., Liou, Y.-A., & Ha, K.-J. (2009). Aerosol effects on the enhancement of cloud-to-ground lightning over major urban areas of South Korea. *Atmospheric Research*, *92*(1), 80–87.

Kar, S. K., & Liou, Y. A. (2014). Enhancement of cloud-to-ground lightning activity over Taipei, Taiwan in relation to urbanization. *Atmospheric Research*, p. *147–148*(May 2014), pp. 111–120. https://doi.org/10.1016/j.atmosres.2014.05.017

Kar, S. K., & Liou, Y.-A. (2019). Influence of land use and land cover change on the formation of local lightning. *Remote Sensing*, *11*(4), 407.

Karger, D. N., Conrad, O., Böhner, J., Kawohl, T., Kreft, H., Soria-Auza, R. W., Zimmermann, N. E., Linder, H. P., & Kessler, M. (2017). Climatologies at high resolution for the earth's land surface areas [Dataset]. *Scientific Data*, *4*, 1–20. https://doi.org/10.1038/sdata.2017.122

Kaufman, Y. J., Tanré, D., & Boucher, O. (2002). *A satellite view of aerosols in the climate system* [Dataset]. *419*(September), 215–223. https://doi.org/10.1038/nature01091

Krotkov, N. A., & Veefkind, P. (2016). OMI/Aura Nitrogen Dioxide (NO2) Total and Tropospheric Column 1-orbit L2 Swath 13x24 km V003 [Dataset]. *Greenbelt, MD, USA, Goddard Earth Sciences Data and Information Services Center (GES DISC)*, *10*.

Lal, D. M., & Pawar, S. D. (2011). Effect of urbanization on lightning over four metropolitan cities of India. *Atmospheric Environment*, *45*(1), 191–196.

Liu, C., & Heckman, S. (2012). Total lightning data and real-time severe storm prediction. *Conference on Meteorological and Environmental Instruments and Methods of Observation.*, pp. 1–12. https://www.wmo.int/pages/prog/www/IMOP/publications/IOM-109_TECO-2012/Session5/P5_10_Liu_Total_Lightning_Data_and_Real-Time_Severe_Storm_Prediction.pdf

Lorenz, C., & Kunstmann, H. (2012). The hydrological cycle in three state-of-the-art reanalyses: Intercomparison and performance analysis. *Journal of Hydrometeorology*, *13*(5), 1397–1420. https://doi.org/10.1175/JHM-D-11-088.1

Lynn, B. H., Yair, Y., Shpund, J., Levi, Y., Qie, X., & Khain, A. (2020). Using Factor Separation to Elucidate the Respective Contributions of Desert Dust and Urban Pollution to the 4 January 2020 Tel Aviv Lightning and Flash Flood Disaster. *Journal of Geophysical Research: Atmospheres*, *125*(24). https://doi.org/10.1029/2020JD033520

Martins, J. A., Silva Dias, M. A. F. da, & Gonçalves, F. L. T. (2009). Impact of biomass burning aerosols on precipitation in the Amazon: A modeling case study. *Journal of Geophysical Research: Atmospheres*, *114*(D2).

Mendez-Espinosa, J. F., Belalcazar, L. C., & Betancourt, R. M. (2019). Regional air quality impact of northern South America biomass burning emissions. *Atmospheric Environment*, 203, 131-140.

Mushtaq, F., Nee Lala, M. G., & Anand, A. (2018). Spatio-temporal variability of lightning activity over J&K region and its relationship with topography, vegetation cover, and absorbing aerosol index (AAI). In *Journal of Atmospheric and Solar-Terrestrial Physics* (Vol. 179). Elsevier Ltd. https://doi.org/10.1016/j.jastp.2018.08.011

Naccarato, K. P., Pinto Jr, O., & Pinto, I. (2003). Evidence of thermal and aerosol effects on the cloud-to-ground lightning density and polarity over large urban areas of Southeastern Brazil. *Geophysical Research Letters*, *30*(13).

Oke, T. R. (1982). The energetic basis of the urban heat island. *Quarterly Journal of the Royal Meteorological Society*, *108*(455), 1–24. https://doi.org/10.1002/qj.49710845502

Orville, R. E., & Huffines, G. R. (1999). Lightning ground flash measurements over the contiguous United States: 1995-97. *Monthly Weather Review*, *127*(11), 2693–2703. https://doi.org/10.1175/1520-0493(1999)127<2693:LGFMOT>2.0.CO;2

474 Orville, R. E., Huffines, G., Nielsen-Gammon, J., Zhang, R., Ely, B., Steiger, S., Phillips, S.,
475 Allen, S., & Read, W. (2001). Enhancement of cloud-to-ground lightning over Houston,
476 Texas. *Geophysical Research Letters*, *28*(13), 2597–2600.
477 https://doi.org/10.1029/2001GL012990

478 Pamarthi, A. (2019). The recent trend of the temperature in major cities of India: A difference
479 between inland areas and coastal areas in the climate change scenario. *Atmospheric science*,
480 1, 1.

481 Pinto Jr., O., Pinto, I. R. C. de A., & Neto, O. P. (2013). Lightning Enhancement in the Amazon
482 Region Due to Urban Activity. *American Journal of Climate Change*, *02*(04), 270–274.
483 https://doi.org/10.4236/ajcc.2013.24026

484 R Core Team. (2013). *R: A language and environment for statistical computing*.

485 Reap, R. M. (1986). American Meteorological Society Evaluation of Cloud-to-Ground Lightning
486 Data from the Western United States for the 1983 – 84 Summer Seasons Author (s):
487 Ronald M . Reap Source : Journal of Climate and Applied Meteorology , Vol . 25 , No . 6 (
488 June 1986. *Journal of Applied Meteorology and Climatology*, *25*(6), 785–799.

489 Rozoff, C. M., Cotton, W. R., & Adegoke, J. O. (2003). Simulation of St. Louis, Missouri, land
490 use impacts on thunderstorms. *Journal of Applied Meteorology*, *42*(6), 716–738.
491 https://doi.org/10.1175/1520-0450(2003)042<0716:SOSLML>2.0.CO;2

492 Shahmohamadi, P., Che-Ani, A. I., Ramly, A., Maulud, K. N. A., & Mohd-Nor, M. F. I. (2010).
493 Reducing urban heat island effects: A systematic review to achieve energy consumption
494 balance. *International Journal of Physical Sciences*, *5*(6), 626–636.

495 Shepherd, J. M., Stallins, J. A., Jin, M. L., & Mote, T. L. (2015). Urbanization: Impacts on
496 clouds, precipitation, and lightning. *Urban Ecosystem Ecology*, *October*, pp. 1–28.
497 https://doi.org/10.2134/agronmonogr55.c1

498 Solargis. (2019). *Global Solar Atlas 2.0. A free web-based application developed and operated*
499 *by the company Solargis s.r.o. on behalf of the World Bank Group, utilizing Solargis data,*
500 *with funding provided by the Energy Sector Management Assistance Program (ESMAP)*
501 [Dataset]. https://globalsolaratlas.info

502 Solomon, S. (2007). The physical science basis: Contribution of Working Group I to the fourth
503 assessment report of the Intergovernmental Panel on Climate Change. *Intergovernmental*
504 *Panel on Climate Change (IPCC), Climate Change 2007*, p. *996*.

505 Song, Y., Semazzi, F. H. M., Xie, L., & Ogallo, L. J. (2004). A coupled regional climate model
506 for the Lake Victoria Basin of East Africa. *International Journal of Climatology*, *24*(1), 57–
507 75. https://doi.org/10.1002/joc.983

Soriano, L. R., & de Pablo, F. (2002). Effect of small urban areas in central Spain on the enhancement of cloud-to-ground lightning activity. *Atmospheric Environment*, *36*(17), 2809–2816.

Steiger, S. M., Orville, R. E., & Huffines, G. (2002). Cloud-to-ground lightning characteristics over Houston, Texas: 1989--2000. *Journal of Geophysical Research: Atmospheres*, *107*(D11), ACL--2.

Stolz, D. C. (2016). The simultaneous influence of thermodynamics and aerosols on deep convection and lightning. In *Colorado State University*. https://minerva-access.unimelb.edu.au/handle/11343/56627%0Ahttp://www.academia.edu/download/39541120/performance_culture.doc

Strikas, O. M., & Elsner, J. B. (2013). Enhanced cloud-to-ground lightning frequency in the vicinity of coal plants and highways in Northern Georgia, USA. *Atmospheric Science Letters*, *14*(4), 243–248.

Thielen, J., Wobrock, W., Gadian, A., Mestayer, P. G., & Creutin, J.-D. (2000). The possible influence of urban surfaces on rainfall development: a sensitivity study in 2D in the meso-γ-scale. *Atmospheric Research*, *54*(1), 15–39.

Thornton, J. A., Virts, K. S., Holzworth, R. H., & Mitchell, T. P. (2017). Lightning enhancement over major oceanic shipping lanes. *Geophysical Research Letters*, *44*(17), 9102–9111. https://doi.org/10.1002/2017GL074982

Twomey, S. A., Piepgrass, M., & Wolfe, T. L. (1984). An assessment of the impact of pollution on global cloud albedo. *Tellus B*, *36*(5), 356–366.

United Nations, D. of E., and S. A. P. D. (2018). *World Urbanization Prospects: The 2018 Revision* [Dataset]. United Nations New York, NY, USA. https://population.un.org/wup/Download/

Wang, C. (2005). A modeling study of the response of tropical deep convection to the increase of cloud condensation nuclei concentration: 1. Dynamics and microphysics. *Journal of Geophysical Research: Atmospheres*, *110*(D21).

Wang, H., Shi, Z., Wang, X., Tan, Y., Wang, H., Li, L., & Lin, X. (2021a). Cloud-to-Ground Lightning Response to Aerosol over Air-Polluted Urban Areas in China. *Remote Sensing*, *13*(13), 2600.

Wang, Y., Wan, Q., Meng, W., Liao, F., Tan, H., & Zhang, R. (2011). Long-term impacts of aerosols on precipitation and lightning over the Pearl River Delta megacity area in China. *Atmospheric Chemistry and Physics*, *11*(23), 12421–12436.

Wang, Y., Lu, G., Shi, T., Ma, M., Zhu, B., Liu, D., Peng, C., & Wang, Y. (2021b). Enhancement of Cloud-to-Ground Lightning Activity Caused by the Urban Effect: A Case Study in the Beijing Metropolitan Area. *Remote Sensing*, *13*(7), 1228.

Westcott, N. E. (1995). Summertime cloud-to-ground lightning activity around major Midwestern urban areas. In *Journal of Applied Meteorology* (Vol. 34, Issue 7, pp. 1633–1642). https://doi.org/10.1175/1520-0450-34.7.1633

Williams, E. R., Zhang, R., & Rydock, J. (1991). Mixed-phase microphysics and cloud electrification. *Journal of the Atmospheric Sciences*, *48*(19), 2195–2203.

Yau, M. K., & Rogers, R. R. (1996). *A short course in cloud physics*. Elsevier.

Table 1. Review of studies investigating the urban lightning enhancement effect. "Response" is the response variable used to measure lightning enhancement reported as lightning strike frequency (km^{-2}), total lightning (in-cloud lightning and lightning strikes, km^{-2}), Z-ratio (lightning strikes/total lightning), or lightning potential index (LPI, J kg^{-1}). "Predictor(s)" refers to the variables that significantly predicted variation in the response reported as PM10 and PM2.5 (Particulate Matter less than 10 μm and 2.5 μm in diameter, respectively), SO_2 (sulfur dioxide concentration), UHI (Urban Heat Island effect), AOD (Aerosol Optical Depth), CAPE (Convective Available Potential Energy), or SRH (surface relative humidity). "Significant enhance." is the fraction of cities that exhibited significant enhancement within each study.

City or region	Response	Significant predictor(s)	Significant enhance.	Reference
São Paulo and nearby cities (Brazil)	Lightning strike frequency	PM10, UHI	3/3	Naccarato *et al*. (2003)
Manaus (Brazil)	Lightning strike frequency	UHI	1/1	Pinto *et al*. (2013)
Pearl River Delta megacity (China)	LPI, Lightning strike frequency	AOD	1/1	Wang *et al.* (2011)
Beijing (China)	Lightning strike frequency	Air temperature, SO_2, NO_2, PM2.5, and PM10	1/1	Wang *et al.* (2021b)
Chengdu, Wuhan, and Jinan (China)	Lightning strike frequency, Z-ratio	CAPE, SRH, and AOD	3/3	Wang *et al.* (2021a)
Delhi, Mumbai, Bengaluru, and Kolkata (India)	Total lightning	AOD, UHI	1/4	Lal and Pawar (2011)
Tel Aviv (Israel)	Total lightning	Aerosol concentration, AOD, PM25, PM10	1/1	Lynn *et al.* (2020)
Seoul (South Korea)	Lightning strike frequency	PM10 and SO_2	1/1	Kar *et al.* (2007)
Busan, Incheon, Daegu, Taejon and Gwangju (South Korea)	Lightning strike frequency	PM10 and SO_2	5/5	Kar *et al.* (2009)

Taipei (Taiwan)	Lightning strike frequency	PM10 and SO_2	1/1	Kar and Liou (2019)
Central Spain	Lightning strike ratio (upwind/downwind)	Population, urban size, PM10 and SO_2	7/9	Soriano and de Pablo (2002)
Midwestern (USA)	Lightning strike frequency	Pollution, topography	12/16	Westcott (1995)
Houston, Texas (USA)	Lightning strike frequency	PM10 and UHI	1/1	Steiger *et al.* (2002)
Northern Georgia (USA)	Lightning strike frequency	Distances from the nearest coal power plant and highways	1/1	Strikas and Elsner (2013)
Charlotte-Atlanta megaregion (USA)	Total lightning	Urban area, density, and orientation.	2/3	Burke and Shepherd (2023)

559

560 **Table 2.** Predictor variables explain the variation of lighting enhancement along with their measurement method, units, and source.
561 All variables were upscaled or downscaled to the spatial grain of the lightning frequency data.

Group	Variable	Units	Temporal resolution (years covered)	Spatial scale	Data type	Source
Climate	Regional lightning frequency	Strikes km^{-2} $year^{-1}$	Monthly total (2013-2020)	0.05 x 0.05	Electrical ground sensor network	Liu and Heckman, 2012
	Average air temperature	K (at 2 meters above the surface from ERA5 data)	Monthly averages of daily data (2013-2019)	0.05 x 0.05	Reanalysis of weather station data	Karger *et al.,* 2017
	Maximum air temperature					
	Minimum air temperature					
	Local precipitation	kg m^{-2} $month^{-1}$	Monthly total (2013-2018)	0.05 x 0.05		Karger *et al.,* 2017
Pollution	Total aerosols	µm of particulates scaled from 0 to 1	Monthly averages (2013-2020)	0.1 x 0.1	Satellite sensors	Kaufman *et al.,* 2002
	NO_2	billion molecules mm^{-2}		0.1 x 0.1		Krotkov *et al.,* 2016
	SO_2	µg m^{-3}		0.625 x 0.5	Reanalysis of satellite data	Gelaro *et al.,* 2017
Topography & Geography	Elevation	m	Single measurement (2018)	3 arcsec (~ 90 m)	Satellite sensors	Solargis, 2019

	Distance to water bodies	km	Single measurement (2021)	0.1 x 0.1	Satellite sensors	Flanders Marine Institute, 2021
Urban chars.	Urban area	km^2	Single measurement (2021)	0.05 x 0.05	Satellite sensors	Friedl and Sulla-Menashe, 2019
	Population	1,000s of inhabitants	Single measurement (2018)	-	Population census	UN, 2018
	Greenspace	% of natural area	Single measurement (2021)	0.05 x 0.05	Satellite sensors	Friedl and Sulla-Menashe, 2019

562

563

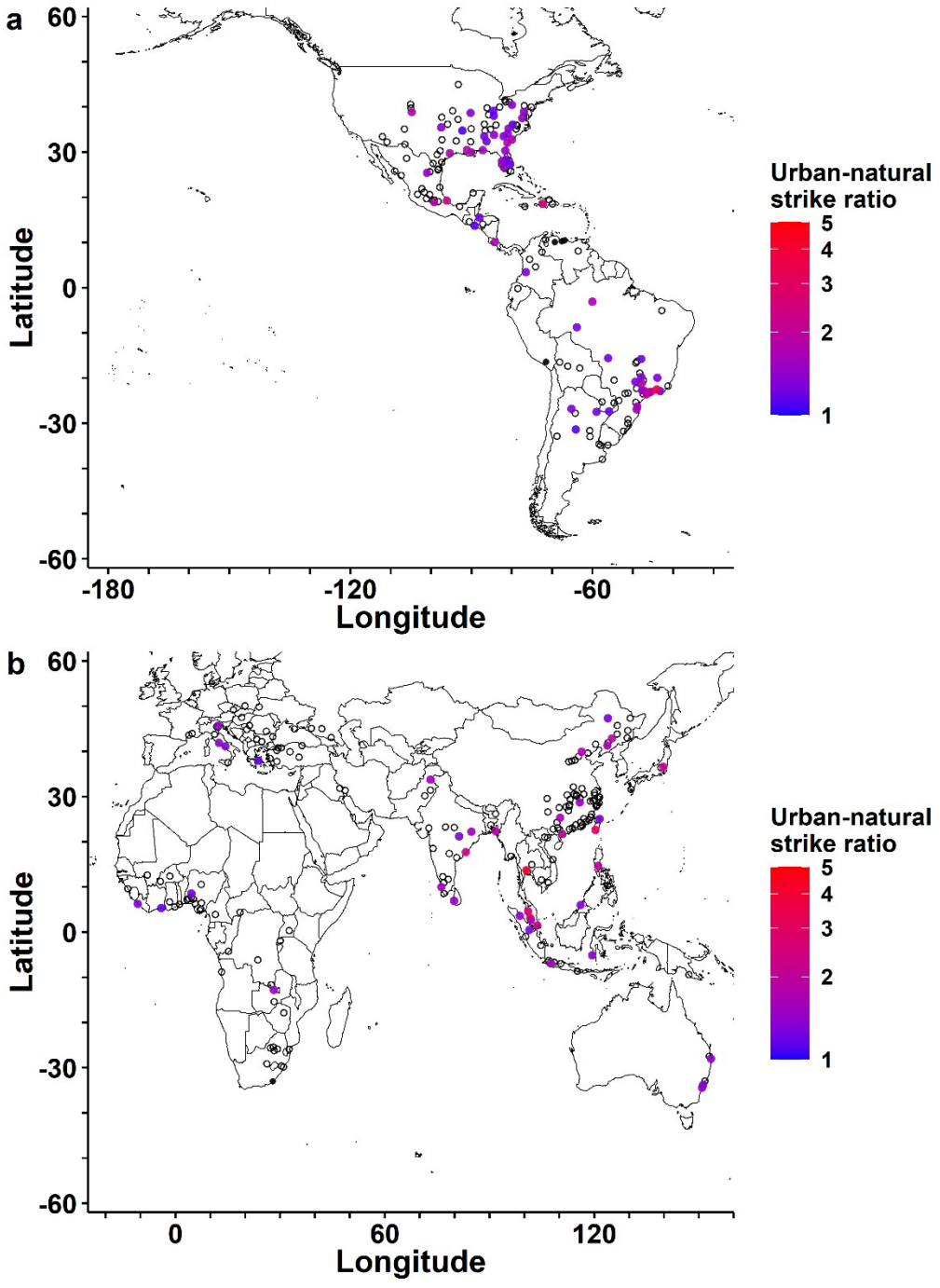

564

565 **Fig. 1.** The global distribution of cities (> 300,000 inhabitants) and variation in the strength of
566 urban lightning enhancement are split approximately between the western hemisphere (panel a)
567 and the Eastern hemisphere (panel b). Black points represent cities with low regional lightning
568 strike frequencies (<1 strike km-2 yr-1), and empty circles represent cities without urban
569 lightning enhancement (<0.5 Glass' delta). Colored points represent cities with significant
570 lightning enhancement (≥0.5 Glass' delta) shaded by the strength of enhancement (i.e., urban-
571 natural strike ratio).

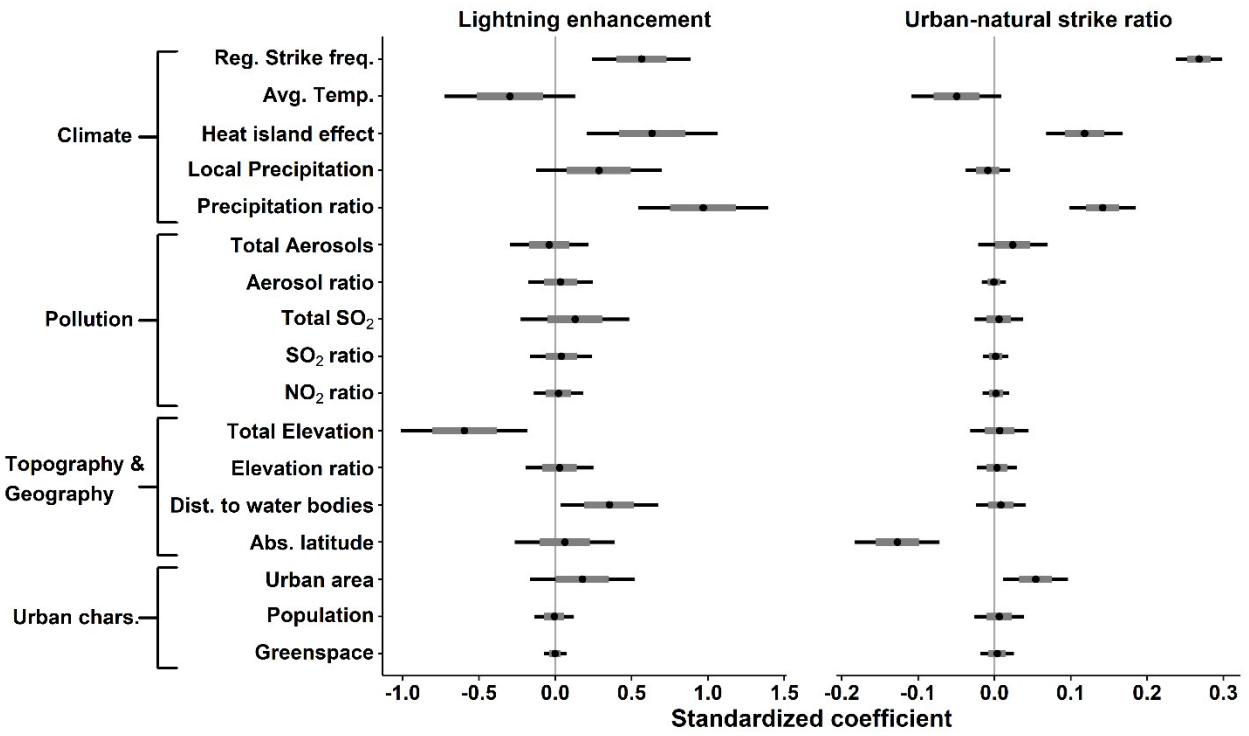

Fig. 2. Model averaged relationships between the likelihood and magnitude of lightning enhancement (i.e., the urban-natural strike ratio) with the different explanatory variables. The black dots are the estimated value of the predictors, the gray bars are their standard error, and the black lines depict their 95% confidence intervals. If the 95% confidence interval for a given term overlaps with the zero line, then that indicates that the modeled effect was not significantly different from zero.

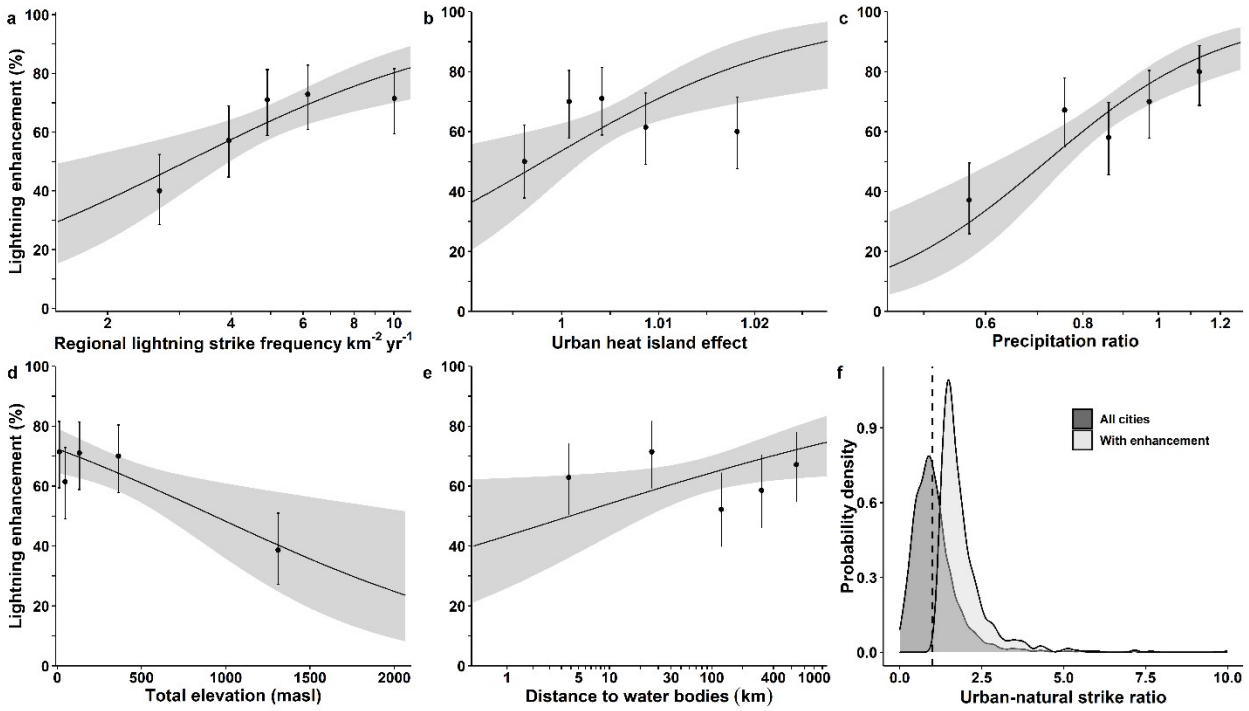

Fig. 3. Variation in lightning enhancement with significant predictors from the AIC model averaging analysis (panel a: regional lightning strike frequency (km^{-2} yr^{-1}); panel b: urban heat island effect; panel c: precipitation ratio; panel d: total elevation (masl); panel e: distance to water bodies). The regression lines represent the model averaging slopes for each predictor and lightning enhancement. The shaded portions represent the 95% confidence interval of each regression line. Lightning enhancement was binned into quantiles to allow visualization of model fit to the binary response variable. Panel f shows a density plot representing the probability density of the urban-natural strike ratio for all cities and cities with unambiguous lightning enhancement. The dashed line represents the value at which urban and natural lightning strike frequency equals.